Open Peer Review on Qeios

Modeling the processive movement of dimerized kinesin-10 NOD motors

Ping Xie[1]

1 Institute of Physics Chinese Academy of Sciences

Funding: No specific funding was received for this work.

Potential competing interests: No potential competing interests to declare.

Abstract

Chromokinesin NOD is a member of kinesin-10 family. It is monomeric in solution, lacking the capacity for movement on microtubules, but when dimerized can move directionally and processively towards microtubule plus ends by hydrolyzing ATP molecules, which is responsible for driving chromosome arms towards the spindle equator during metaphase of mitosis. Prior experimental data showed puzzlingly that the NOD head in nucleotide-free state has a high affinity to microtubule, whereas in any nucleotide-bound state has a low affinity. Due to these puzzling experimental data, it is perplexing how the dimerized NOD motor can move directionally and processively on microtubule. Here, based on the peculiar characteristic of the nucleotide-dependent affinity of the NOD head to microtubule and inspired by previously proposed models for better-studied dimeric kinesin-1 motors, three models are presented for the processive movement of the dimerized NOD motor, with which the dynamics of the motor is studied theoretically. The theoretical results with one of the three models can explain well the directional and processive movement of the NOD dimer. Furthermore, predicted results with the model are provided. In addition, a similar model is presented for the directional and processive movement of another species of kinesin-10 chromokinesin—dimerized human KID.

Ping Xie*

Key Laboratory of Soft Matter Physics, Institute of Physics, Chinese Academy of Sciences, Beijing 100190, China

*Email address: pxie@aphy.iphy.ac.cn

Keywords: molecular motor; chromokinesin; processivity; chemomechanical coupling.

1. Introduction

Kinesins constitute a superfamily of motor proteins, including kinesin-1 through kinesin-14 families and ungrouped orphan family [1]. They perform various functions such as cargo transport, regulation of microtubule (MT) dynamics, chromosome

segregation during mitosis, etc., in cells [2]. The Drosophila melanogaster chromokinesin NOD is a member of kinesin-10 family [3][4]. Sequence, structure and kinetic studies indicated that in solution NOD is in the monomeric form, lacking the capacity for movement on MT [5][6]. NOD consists of an N-terminal catalytic domain (also called head) that can bind to MT and catalyze the ATPase activity, like kinesin-1 head, and a C-terminal DNA-binding domain that can bind the chromosome arms [7]. Like other species of kinesin-10 motors such as human KID, NOD is essential for generating the polar ejection force that guides chromosome arm congression during metaphase of mitosis [3][4][8]. In the absence of MT the NOD head has a very low ATPase activity, and the presence of MT stimulates significantly the ATPase activity [9]. In nucleotide-free state the NOD head has a high affinity to MT, whereas in any nucleotide-bound state such as AMPPNP (a non-hydrolyzable ATP analog) or ADP state the NOD head has a weak affinity to MT [5][9]. This characteristic for the NOD head is in sharp contrast to that for the kinesin-1 head which shows the weak affinity in ADP state while in other nucleotide states such as nucleotide-free and AMPPNP states has the high affinity to MT [10][11]. Interestingly, recent in vivo studies showed that after dimerization NOD can move directionally and processively on MT towards the plus end [12] and thus can perform the function of driving chromosome arms towards the spindle equator. This feature for the NOD protein is similar to that for members of kinesin-3 family which are also in the monomeric form and inactive in motility in solution but become motile with a high processivity after dimerization induced by the cargo binding [13][14].

However, the mechanism of the processive movement of the dimerized NOD motor is unknown. In particular, considering that the NOD head in any nucleotide-bound state has a weak affinity to MT, it is perplexing how the dimerized NOD motor can move processivly on MT. To understand the underlying physical mechanism, inspired by previously proposed models for better-studied dimeric kinesin-1 motors (see, e.g., recent review article [15]) we propose three models here for the dimerized NOD motor, based on which the dynamics of the motor is studied theoretically. The theoretical results obtained with two of the three models show that the motor is nonprocessive while the theoretical results obtained with the third model explain well the directional and processive movement of the motor. Moreover, predicted results on load dependences of velocity and run length of the motor obtained with the third model are provided, which can be tested in future using single molecule optical trapping methods.

2. Models

2.1. Model 1

Analogous to the prevailing model presented in the literature for the stepping of kinesin-1 motor on MT, where it was proposed that the docking of the neck linker (NL) onto the leading head induced by ATP binding generates the force to drive the forward movement of the motor [16][17][18][19][20][21], a model (called Model 1) for the stepping of dimerized NOD motor is presented here. Model 1 is constructed based mainly on following two elements. (i) As the prior biochemical data showed, the NOD head in nucleotide-free state has a high binding energy to MT while in any nucleotide-bound state (ATP, ADP.Pi or ADP state) has a low binding energy [5][9]. (ii) As in the case of kinesin-1, it is argued that when the NOD head is in ATP and ADP.Pi states its NL can dock onto the head in the forward or MT-plus-end direction, while when the

NOD head is in ADP and nucleotide-free states its NL is undocked, although the available structural data indicated that the NL of the NOD head in both AMPPNP and ADP states could be undocked [5].

In Model 1, it is proposed that upon ATP binding to the nucleotide-free NOD head, the head detaches from MT, which is consistent with the available experimental data showing that after ATP binding the NOD head detaches easily from MT [5][9]. This is similar to the previous proposal for kinesin-1, where after transition from the strong MT-binding state (e.g., ATP or ADP.Pi state) to weak MT-binding state (i.e., ADP state) the head detaches from MT [21]. Model 1 is schematically illustrated in Fig. 1. We begin the chemomechanical coupling pathway of the dimerized NOD motor with the leading head in nucleotide-free state bound strongly to MT and the trailing head in ATP state detached from MT and located in the rear position relative to the leading head (or fluctuated around the MT-bound head) (Fig. 1a), similar to the prior proposal for the kinesin-1 dimer [21]. For the case of the kinesin-1, due to the head in ATP state having a high affinity to MT [10][11], it was argued that the NL docking induced by ATP binding to the leading head bound strongly to MT drives the detached head in ADP (or weak MT-binding) state to move to the front position and then confines the detached ADP-head in the vicinity of the front tubulin. The detached ADP-head with an undocked NL binds to the front tubulin. This results in a forward step of the kinesin-1 motor. However, for the case of the NOD motor, since the available experimental data showed that after ATP binding to the nucleotide-free NOD head bound to MT the ATP-head detaches easily from MT [5][9], ATP binding to the leading head results in the detachment of the leading head and thus the detachment of the NOD dimer (Fig. 1b). Clearly, Model 1 cannot explain the processive movement of the NOD dimer.

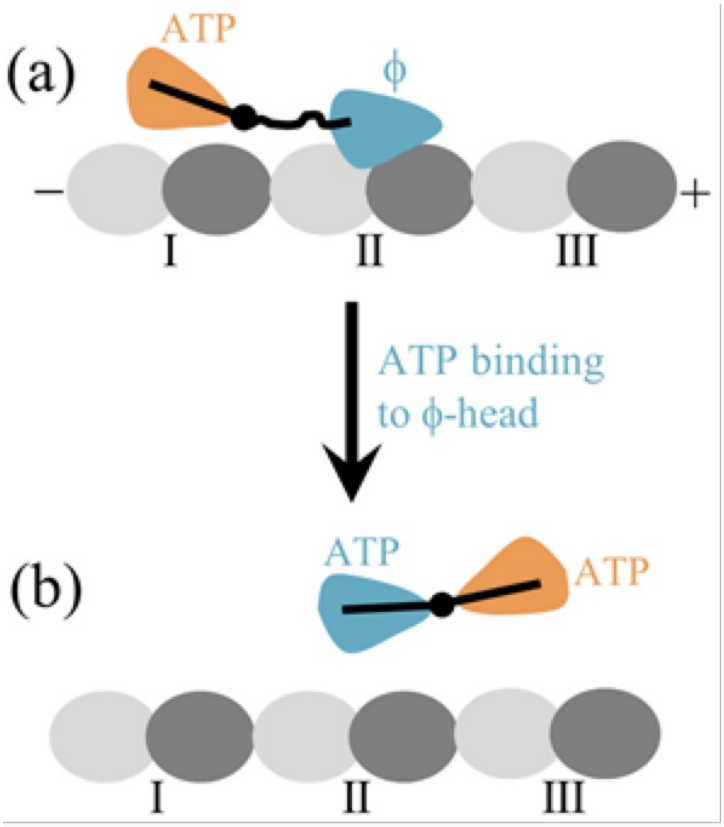

Fig. 1. Model 1 for stepping of dimerized NOD motor. (a, b) The chemomechanical coupling pathway (see Section 2.1 for detailed descriptions). The nucleotide-free state is denoted by ϕ.

2.2. Model 2

Similar to the prevailing model for the kinesin-1 motor, where the NL docking drives the forward movement of the motor [16][17][18][19][20], another model (called Model 2) for the stepping of the dimerized NOD motor is proposed here. Model 2 is constructed still based mainly on the two elements described in Model 1.

In Model 2, it is proposed that only under the force, which for example is generated by NL docking, can the NOD head in weak MT-binding (or nucleotide-bound) state be driven to detach from MT. Model 2 is schematically illustrated in Fig. 2, where for simplicity ATP represents both ATP and ADP.Pi. We begin the stepping pathway with the trailing head in ATP state bound weakly to tubulin I in a MT filament and the leading head in nucleotide-free state bound strongly to tubulin II (Fig. 2a). Then, three scenarios can occur. The first scenario is that ATP binding to the leading head occurs before ATP transition to ADP in the trailing head, which corresponds to the case of saturating or physiological ATP concentrations. The second scenario is that ATP binding to the leading head occurs after ATP transition to ADP but before ADP release in the trailing head, which corresponds to the case of medium ATP concentrations. The third scenario is that ATP binding to the leading head occurs after ATP transition to ADP and then ADP release in the trailing head, which corresponds to the case of low ATP concentrations.

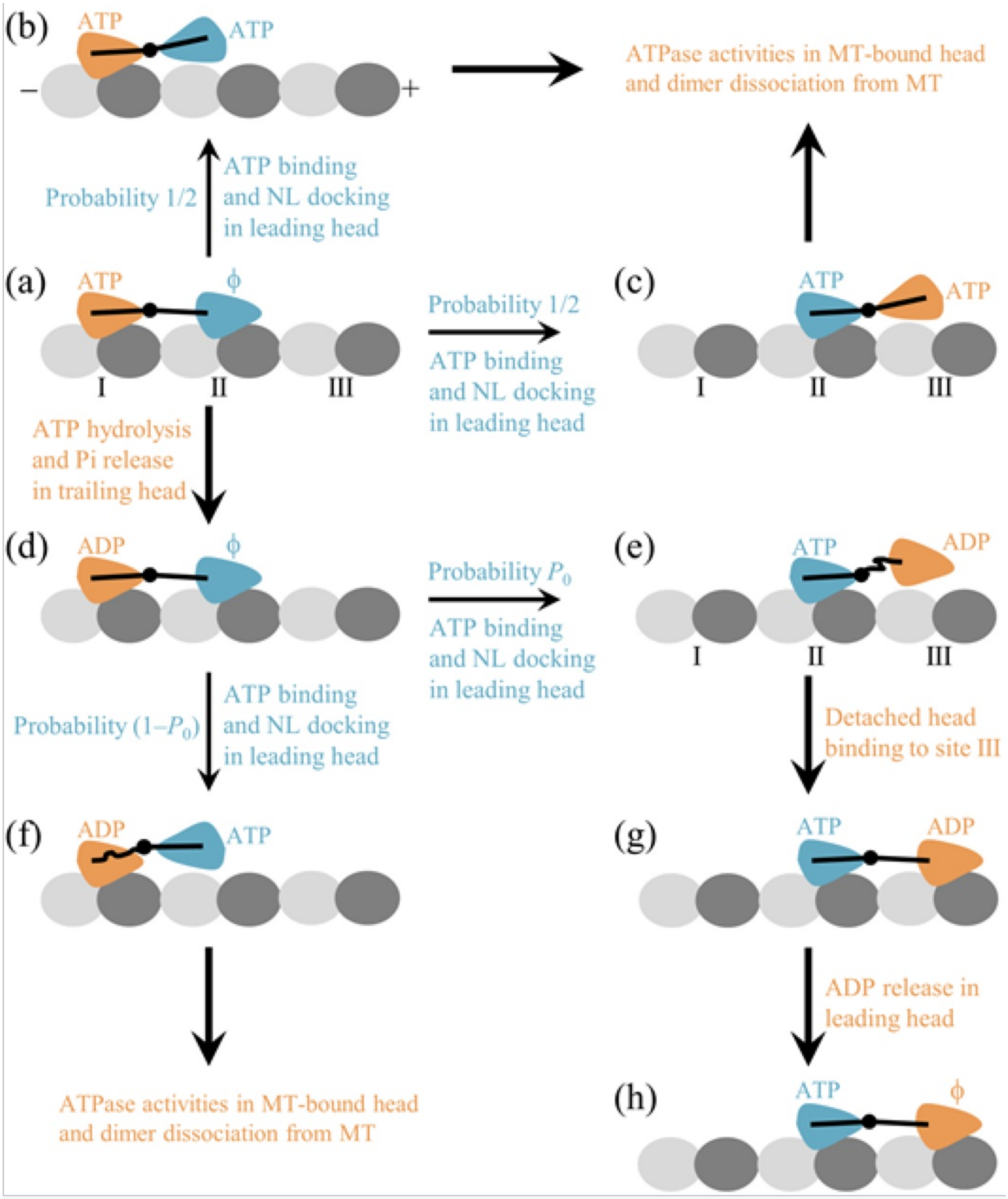

Fig. 2. Model 2 for stepping of dimerized NOD motor. (a – h) The chemomechanical coupling pathway (see Section 2.2 for detailed descriptions). The nucleotide-free state is denoted by ϕ, and for simplicity, both ATP and ADP.Pi states are represented by ATP state.

For the first scenario, after ATP binding the leading head becomes bound weakly to tubulin II. The NL docking of the leading head can either drive the leading ATP-head to detach from tubulin II and then move to the equilibrium position

relative to the other MT-bound ATP-head (Fig. 2b) or drive the trailing ATP-head to detach from tubulin I and then move to the equilibrium position relative to the MT-bound ATP-head (Fig. 2c). Since from Fig. 2a both the transition to Fig. 2b and that to Fig. 2c overcome the same weak binding energy of one ATP-head to MT, each of the two transitions occurs with the same probability 1/2. In Fig. 2b and c, with the docked NL the detached ATP-head cannot bind to MT, and its ATPase activity can be neglected because the biochemical data showed that the ATPase activity of a head not bound to MT is very low [9]. Although the ATPase activity (including ATP hydrolysis, Pi release, ADP release and then ATP binding) can occur in the MT-bound head in Fig. 2b and c, the motor cannot make the directional movement on MT. Finally, the dimer dissociates from MT by overcoming the weak binding energy of the head to MT in ATP, ADP.Pi or ADP state. Thus, the model for the first scenario cannot explain the processive movement of the NOD dimer.

Then, consider the second scenario that ATP binding to the leading head occurs after ATP transition to ADP but before ADP release in the trailing head (Fig. 2d, e and f). After ATP binding the leading head becomes bound weakly to tubulin II. The NL docking of the leading head can either (with probability P_0) drive the trailing ADP-head to detach from tubulin I and then move to the forward position relative to the MT-bound ATP-head (Fig. 2e) or (with probability $1–P_0$) drive the leading ATP-head to detach from tubulin II and then move to the equilibrium position relative to the other MT-bound ADP-head (Fig. 2f). Since the biochemical data of Cochran et al. [5] showed that the NOD head in ADP state has the nearly same weak affinity to MT as in ATP state, from Fig. 2d both the transition to Fig. 2e and that to Fig. 2f overcome the nearly same weak binding energy of one head to MT. Thus, the two transitions occur with nearly equal probability, namely with $P_0 \approx 1/2$. In Fig. 2f, although the ATPase activity can occur in the MT-bound head, the detached ATP-head with docked NL cannot bind to the front tubulin II. Thus, the motor cannot make the directional movement toward the plus end of MT and finally the MT-bound head dissociates from MT by overcoming the weak binding energy to MT in ATP, ADP.Pi or ADP state. In Fig. 2f, a possibly alternative transition is that the detached ATP-head can bind to the minus-ended tubulin adjacent to tubulin I because the NL of the MT-bound ADP-head is undocked, which is followed by ADP release from the new leading head, the dimer making a backward step (not shown in Fig. 2). In Fig. 2f, the former transition is called transition 2a while the latter transition is called transition 2b. In Fig. 2e, the undocked NL allows the detached ADP-head to bind weakly to the nearest tubulin III (Fig. 2g). ADP is then released from the leading head (Fig. 2h). Fig. 2h is the same as Fig. 2a except that the dimer made a forward step. The processive movement of the motor for the second scenario will be studied later in Section 3.1.

Last, consider the third scenario that ATP transition to ADP and then ADP release in the trailing head occur before ATP binding to the leading head, with both heads becoming nucleotide free (not shown in Fig. 2). Then, if ATP binding to the leading head occurs before ATP binding to the trailing head, the NL docking of the leading head drives the detachment of the leading head because the nucleotide-free trailing head is bound strongly to MT. Thus, the motor cannot move forward. If ATP binding to the trailing head occurs before ATP binding to the leading head, the system returns to Fig. 2a. Therefore, the model for the third scenario also cannot explain the directional movement of the NOD dimer.

2.3. Model 3

Inspired by the model for kinesin-1 motor, where the forward stepping of the motor is mainly via the Brownian ratchet mechanism [15][22], a model (called Model 3) for the processive stepping of the dimerized NOD motor is proposed here. Model 3 is constructed based mainly on the following elements. (i) The NOD head in nucleotide-free state has a strong interaction with MT while in nucleotide-bound state has a weak interaction, as the biochemical data showed [5][9]. The strong interaction induces very rapidly (with a timescale of the order of 10 – 100 ns) large conformational changes of the local tubulin while the weak interaction induces little conformational changes, as structural and all-atom molecular dynamics simulation studies showed for the kinesin-1 head [23][24][25]. The NOD head in nucleotide-bound state has a much weaker affinity (E_{w1}) to the local tubulin having the large conformational changes than the weak affinity (E_{w2}) to other tubulins without the large conformational changes, as all-atom molecular dynamics simulations showed for the kinesin-1 head [24][25]. This indicates that after ATP binding to the nucleotide-free NOD head, a very short time t_r (in the order of μs) is present when the local tubulin has a very weak affinity E_{w1} to the nucleotide-bound head and in t_r, with the local tubulin restoring elastically to the normally unchanged form, its affinity to the nucleotide-bound head changes to E_{w2}, as argued for kinesin-1 [15][22][24][25]. (ii) Since the structural data showed that AMPPNP binds much more tightly than ADP to the nucleotide-binding site of the NOD head [5], the release of ATP prior to its transition to ADP can be neglected. Moreover, it is argued that the NOD head with the backward-directed NL has a much slower ATPase rate than with the forward-directed NL, similar to the kinesin-1 head, as evidenced as follows. The structural data of the kinesin-1 head showed that the forward-directed NL clashes with a nucleotide-binding motif (a P-loop subdomain) in the nucleotide-free orientation, indicating that the P-loop subdomain is in the ATP-like orientation [26]. This would accelerate significantly the ATPase activity, as biochemical data for the kinesin-1 and kinesin-3 Kif1a heads showed [26][27].

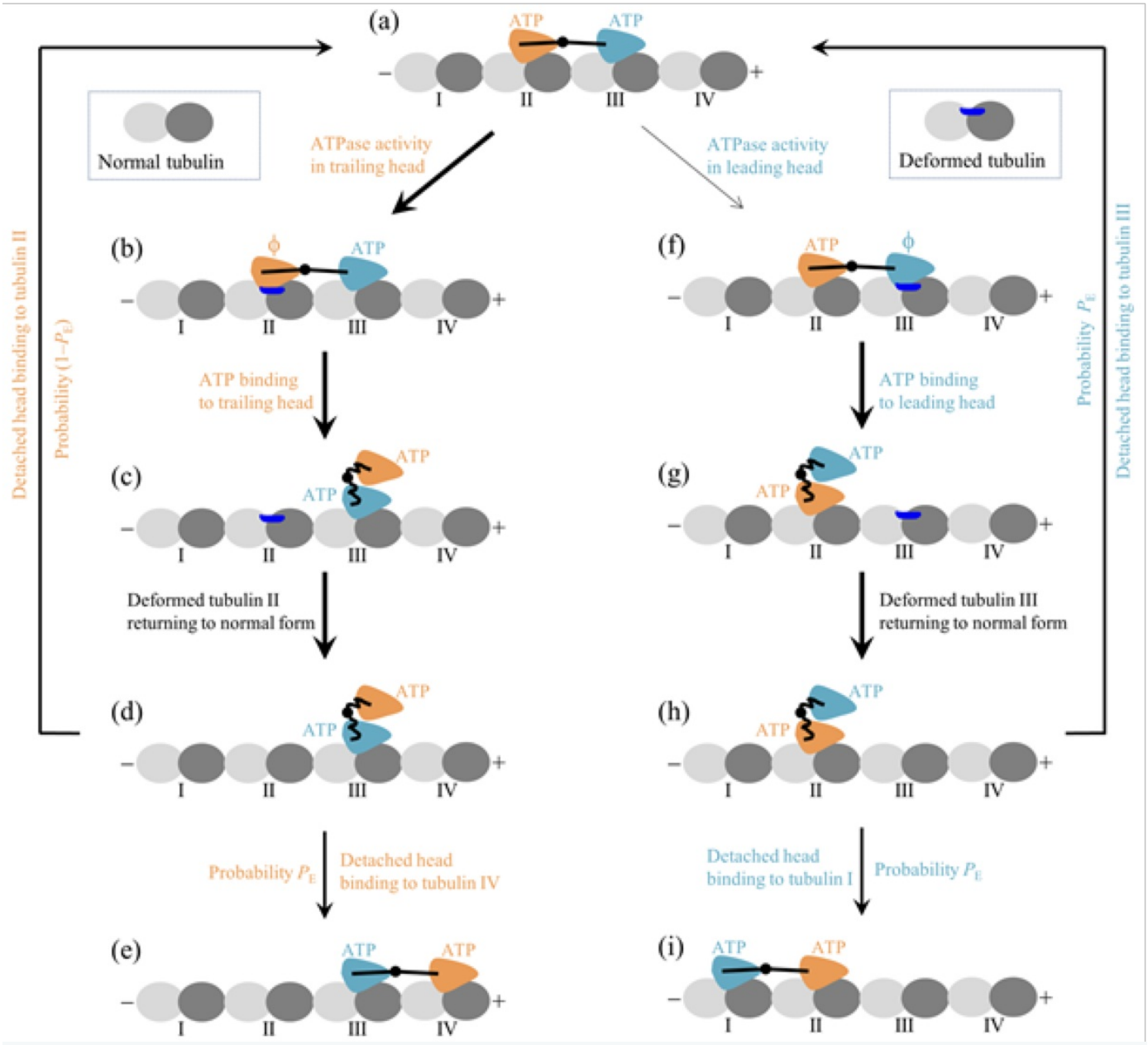

Fig. 3. Model 3 for stepping of dimerized NOD motor. (a) – (i) The chemomechanical coupling pathway (see Section 2.3 for detailed descriptions). Since in nucleotide-bound state (ATP, ADP.Pi or ADP state) the NOD head binds weakly to MT, for simplicity, we use ATP here to represent ATP, ADP.Pi and ADP. The nucleotide-free state is denoted by ϕ. The thickness of the arrow indicates the relative magnitude of the probability of the transition between two states connected by the arrow under no load.

Model 3 is schematically illustrated in Fig. 3, where we focus on high or physiological ATP concentrations (e.g., 1 mM), as used in the experiments of Ye et al. [12], and for simplicity ATP represents ATP, ADP.Pi and ADP. We begin the stepping pathway with both the trailing and leading heads in nucleotide-bound state bound with affinity E_{w2} to tubulins II and III on a MT filament, respectively (Fig. 3a).

First, consider the ATPase activity (including ATP hydrolysis, Pi release and ADP release) taking place in the trailing head. The trailing head in nucleotide-free state becomes bound strongly to tubulin II, inducing very rapidly the large conformational changes of the local tubulin II (Fig. 3b). After ATP binding, the trailing head detaches easily from tubulin II

by overcoming the very small affinity E_{w1} and diffuses forward (Fig. 3c). Note here that the finite length of NL prevents the detached head from diffusing backward and binding to tubulin I. In the short time t_r (in the order of μs), the deformed tubulin II returns elastically to the normal one without the large conformational changes (Fig. 3d). The detached head can diffuse forward further and bind to tubulin IV with affinity E_{w2} that is much larger than E_{w1} (Fig. 3e). From Fig. 3d, the detached head can also diffuse backward and bind to tubulin II with affinity E_{w2} (Fig. 3a). From Fig. 3a to d to e, the dimer takes a forward step by consuming an ATP. From Fig. 3a to d to a, the dimer does not move although an ATP is consumed.

Second, consider the ATPase activity taking place occasionally in the leading head. The leading head in nucleotide-free state becomes bound strongly to tubulin III, inducing very rapidly the large conformational changes of the local tubulin III (Fig. 3f). After ATP binding, the leading head detaches easily from tubulin III by overcoming the very small affinity E_{w1} and diffuses backward (Fig. 3g). In the short time t_r, the deformed tubulin III returns elastically to the normal one without the large conformational changes (Fig. 3h). The detached head can diffuse backward further and bind to tubulin I with affinity E_{w2} (Fig. 3i). From Fig. 3h, the detached head can also diffuse forward and bind to tubulin III with affinity E_{w2} (Fig. 3a). From Fig. 3a to h to i, the dimer takes a backward step by consuming an ATP. From Fig. 3a to h to a, the dimer does not move although an ATP is consumed.

Note that in Model 3 it is implicitly considered that the NL is undocked in any nucleotide state of the head. This is consistent with the available structural data indicating that the NL of the NOD head in both AMPPNP and ADP states could be undocked [5].

3. Results

3.1. Model 1 and Model 2 give nonprocessivity of dimerized NOD motor

The available biochemical data for the single NOD head showed that after mixing of the ATP-head with MT the ATP-head binds rapidly to MT, stimulating the ATPase activity, whereas after ATP binding to the nucleotide-free head bound to MT the ATP-head dissociates easily from MT [5][9]. Then, a puzzling issue is that while after mixing of the ATP-head with MT the ATP-head can bind rapidly to MT, why after ATP binding to the nucleotide-free head the ATP-head can dissociate rapidly from MT. Since in Model 1 and Model 2 the ATP-head has a constant weak affinity to MT, namely has the same weak affinity to MT during the period immediately after ATP binding to the nucleotide-free MT-bound head as that during the period immediately after the ATP-head binding to MT, the puzzling issue is difficult to explain.

As mentioned in Section 2.1, Model 1 cannot explain the processive movement of the NOD dimer. In Model 2, for the first scenario that ATP binding to the leading head occurs before ATP transition to ADP in the trailing head, which corresponds to the case of high or physiological ATP concentrations, the motor cannot make the processive movement, as mentioned in Section 2.2. In Model 2, for the third scenario that ATP transition to ADP and then ADP release in the trailing head occur before ATP binding to the leading head, which corresponds to the case of low ATP concentrations, the motor also

cannot make the processive movement, as mentioned in Section 2.2. Now, consider in Model 2 the second scenario that ATP binding to the leading head occurs after ATP transition to ADP but before ADP release in the trailing head, which corresponds to the case of medium ATP concentrations. From the pathway (Fig. 2a and d – h), for the transition 2a (see Section 2.2), it is noted that on average the number of the forward steps that the motor can take before dissociation can be calculated by $N = \sum_{i=1}^{\infty} \left(P_0\right)^i = P_0/\left(1 - P_0\right)$. As mentioned in Section 2.2, $P_0 \approx 1/2$. Thus, we have $N \approx 1$, implying that the motor cannot move processively on MT. For the transition 2b (see Section 2.2), it is noted that by hydrolyzing one ATP the number of the net forward step is $P_0 - \left(1 - P_0\right) \approx 0$, implying that the motor cannot make the directional movement. Therefore, for either transition 2a or transition 2b in the second scenario, the motor cannot make the directionally processive movement. Taken together, for any scenario, i.e., whether at high, medium or low ATP concentrations, Model 2 gives the non-processive movement of the motor, which is not applicable to the dimerized NOD motor.

3.2. Model 3 explains processivity of dimerized NOD motor

Based on Model 3, the puzzling issue mentioned in the above section can be easily explained as follows. After mixing of the ATP-head with MT, the ATP-head binds rapidly to MT with the affinity E_{w2}, and during the ensuing period of ATP hydrolysis, Pi release and ADP release, the head keeps the affinity E_{w2} to MT. The affinity E_{w2} ensures the head not to be dissociated easily from MT during the ATPase activity. After ADP release, the strong interaction between the nucleotide-free head and the local tubulin induces very rapidly the large conformational changes of the tubulin. After ATP binding to the nucleotide-free head, the ATP-head can dissociate easily by overcoming the very weak affinity E_{w1} to the tubulin having the large conformational changes within time t_r.

Now, we study the stepping dynamics of the dimerized NOD motor. We focus on high or physiological ATP concentrations, as used in the experiments of Ye et al. [12]. We denote by $k^{(+)}$ the ATPase rate of the trailing head with the forward-directed NL and by $k^{(-)}$ the ATPase rate of the leading head with the backward-directed NL. Based on the pathway (Fig. 3), it is noted that for the dimer, during its processive motion the ATPase rates of the trailing and leading heads are $k_T = k^{(+)}$ and $k_L = k^{(-)}$, respectively. As shown in Fig. 3, denote by P_E the probability for the motor to take a forward step after an ATPase activity taking place in the trailing head (i.e., the probability of an effective chemomechanical coupling cycle), with $1–P_E$ being the probability for the motor not to move after an ATPase activity taking place in the trailing head (i.e., the probability of a futile chemomechanical coupling cycle). Correspondingly, the probability for the motor to take a backward step after an ATPase activity taking place in the leading head is $1–P_E$ and the probability for the motor not to move after an ATPase activity taking place in the leading head is P_E. Thus, the velocity of the motor can be written as $v = \left[k_T P_E - k_L\left(1 - P_E\right)\right]d$, where d = 8 nm is the distance between two successive tubulins on a MT filament. The forward to backward stepping ratio (simply called stepping ratio) can be written as $r = k_T P_E/\left[k_L\left(1 - P_E\right)\right]$. With $k_T = k^{(+)}$ and $k_L = k^{(-)}$, the velocity and stepping ratio can be rewritten as

$$v = \left[k^{(+)}P_E - k^{(-)}\left(1 - P_E\right)\right]d, \qquad (1)$$

$$r = \frac{k^{(+)}P_E}{k^{(-)}\left(1 - P_E\right)} \qquad (2)$$

The equation for the load dependence of probability P_E can be derived as follows. After ATP binding to the trailing head, within time t_r the head detaches from tubulin II and diffuses to an intermediate position (Fig. 3c). Since t_r is very short (in the order of μs), within t_r the diffusing ATP-head can rarely reach the next unoccupied tubulin IV. After t_r, the detached ADP-head can either diffuse further forward and bind to tubulin IV or diffuse backward and bind to the previous tubulin II with binding energy E_{w2}. From the intermediate position, under a backward load (F < 0) the ratio of the rate of the detached head diffusing forward and binding to tubulin IV to that of diffusing backward and binding to tubulin II can be approximately written as $k_{Fwd}/k_{Bwd} = \exp\left(\beta F d_1\right)$, where $\beta^{-1} = k_B T$ is the Boltzmann constant times the absolute temperature and d_1 is the force-sensitivity distance for the backward load. The probability P_E can then be calculated by $P_E = k_{Fwd}/\left(k_{Fwd} + k_{Bwd}\right)$, which can be rewritten as

$$P_E = \frac{\exp\left(\beta F d_1\right)}{\exp\left(\beta F d_1\right) + 1}. \qquad (3)$$

Similarly, under a forward load (F > 0) P_E can be written as $P_E = \exp\left(\beta F d_2\right)/\left[\exp\left(\beta F d_2\right) + 1\right]$, where d_2 is the force-sensitivity distance for the forward load. For simplicity, we take $d_2 \approx d_1$ and thus under both backward and forward loads P_E can be written in the same form of Eq. (3).

Substituting Eq. (3) into Eqs. (1) and (2), we have

$$v = \frac{1}{\exp\left(\beta F d_1\right) + 1}\left[k^{(+)}\exp\left(\beta F d_1\right) - k^{(-)}\right]d, \qquad (4)$$

$$r = \frac{k^{(+)}}{k^{(-)}}\exp\left(\beta F d_1\right). \qquad (5)$$

From Eq. (4) and (5) it is noted that under no load, we have velocity $v_0 = \left(k^{(+)} - k^{(-)}\right)d/2$ and stepping ratio $r_0 = k^{(+)}/k^{(-)}$. The available experimental data gave the unloaded velocity v_0 = 7.63 μm/min for the dimerized NOD motor[12]. Thus, we obtain $k^{(+)} - k^{(-)} = 31.8\ s^{-1}$ for the dimerized NOD motor. The available biochemical data showed that the deletion of the NL reduces the ATPase rate of the single kinesin-1 head by about 60-fold relative to the wild-type case [26]. Since the deletion of the NL is equivalent to the NL not in the forward orientation, the biochemical data thus imply that for the kinesin-1 head, $k^{(-)}$ is about 60-fold smaller than $k^{(+)}$. Since no experimental data is available for the relation between $k^{(-)}$ and $k^{(+)}$ for the NOD head. Here, we also take $k^{(-)} = k^{(+)}/60$ for the NOD head, giving the unloaded stepping ratio $r_0 = k^{(+)}/k^{(-)} = 60$ for the dimerized motor. With $k^{(+)} - k^{(-)} = 31.8\ s^{-1}$ and $k^{(-)} = k^{(+)}/60$, we have $k^{(+)} = 32.34\ s^{-1}$ and $k^{(-)} =$

0.54 s^{-1}. From Eqs. (4) and (5) it is seen that to calculate the velocity and stepping ratio under load F, the value of parameter d_1 is also required. Since the value of d_1 is unavailable experimentally, here we take it to be variable. The theoretical results of the velocity and stepping ratio versus F for different values of d_1 are shown in Fig. 4. As expected, a large d_1 has a more sensitive effect on curve of velocity versus F and that of stepping ratio versus F than a small d_1. The velocity decreases with the increase in the magnitude of the backward load and plateaus at the high backward load, with the maximum backward velocity of $k^{(-)}d$ = –0.26 μm/min (Fig. 4a). The velocity increases with the increase in the magnitude of the forward load and plateaus at the high forward load, with the maximum forward velocity of $k^{(+)}d$ = 15.52 μm/min being about 2-fold larger than the unloaded velocity of 7.63 μm/min (Fig. 4a). It is noted that this feature of the load-velocity curve for the NOD motor (Fig. 4a) is similar to that for kinesin-7 CENP-E motor determined experimentally before [28], with both motors being involved in the chromosome congression[3][4][8][29].

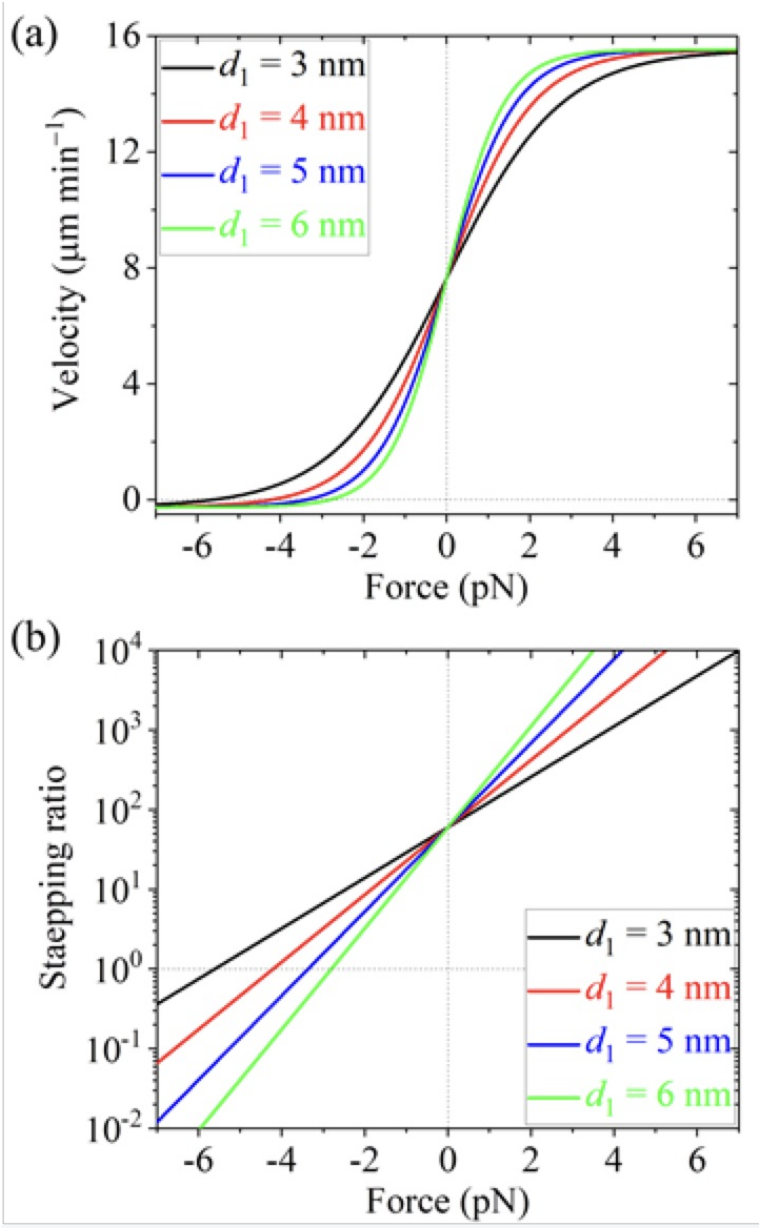

Fig. 4. Theoretical results for load dependences of velocity and stepping ratio for NOD motor obtained on the basis of Model 3. (a) Velocity versus load for

different values of d_1. (b) Stepping ratio versus load for different values of d_1.

Then, we study the run length. In a chemomechanical coupling cycle of the dimerized NOD motor, since the moving time of the detached head relative to the MT-bound head is very short (shorter than 10 μs, as shown previously using Brownian dynamics simulations [30]), the motor is almost always in the state with two heads bound to MT, with the total binding energy of $2E_{w2}$ at saturating ATP. Although E_{w2} is low, the larger $2E_{w2}$ ensures the dimerized motor to dissociate from MT with a low probability in a chemomechanical coupling cycle. Thus, the motor can move processively on MT. Considering that the potential of interaction between the NOD head and MT is approximately symmetrical with respect to the loading direction, as determined before for the kinesin-1 head [31][32], according to Kramers, the load dependence of the dissociation rate of the motor can be approximately written as

$$\varepsilon = \varepsilon_0 \exp(\beta |F| \delta), \qquad (6)$$

where ε is the dissociation rate under no load and δ is the force-sensitivity distance. The run length can then be calculated by

$$L = \frac{v}{\varepsilon} \qquad (7)$$

Substituting Eqs. (4) and (6) into Eq. (7), we obtain

$$L = \frac{k^{(+)}\exp\left(\beta F d_1\right) - k^{(-)}}{\varepsilon_0 \exp(\beta |F| \delta)\left[\exp\left(\beta F d_1\right) + 1\right]} d. \qquad (8)$$

From Eq. (8), it is noted that under no load, the run length has the form, $L_0 = 0.5\left(k^{(+)} - k^{(-)}\right)d/\varepsilon_0$, with L_0 being inversely proportional to ε_0. For example, L_0 = 1272 nm for $\varepsilon_0 = 0.1\ s^{-1}$, where $k^{(+)} - k^{(-)} = 31.8\ s^{-1}$ (see above). The ratio of the run length under load F to the unloaded run length or the run length under load normalized by the unloaded run length, $R_L = L/L_0$, has the form

$$R_L = \frac{2\left[k^{(+)}\exp\left(\beta F d_1\right) - k^{(-)}\right]}{\left(k^{(+)} - k^{(-)}\right)\exp(\beta |F| \delta)\left[\exp\left(\beta F d_1\right) + 1\right]}. \qquad (9)$$

From Eq. (9) it is seen that the curve of ratio RL versus F depends only on parameters $k^{(+)}$, $k^{(-)}$, d_1 and δ. As mentioned above, we have $k^{(+)} = 32.34\ s^{-1}$ and $k^{(-)} = 0.54\ s^{-1}$. Here, we take values of d_1 and δ to be variable. The theoretical results of ratio RL versus F for different values of d_1 and δ are shown in Fig. 5. As expected, for a given set of values of d_1 and δ, the ratio RL decreases with the increase in the magnitude of the backward load. For the small value of d_1 or large value of δ, the ratio RL also decreases with the increase of the forward load. Interestingly, for the large value of d_1 or small value of δ, under a small forward load the run length is larger than the unloaded run length. In addition, Eq. (6) implies that the dissociation time is symmetrical with respect to the loading direction for the NOD motor, which is similar to that for the

kinesin-7 CENP-E motor determined experimentally before [28], with both motors being involved in the chromosome congression [3][4][8][29].

In short, the studies in this section show that Model 3 can be applicable to the dimerized NOD motor. Moreover, the predicted results are provided for load dependences of the velocity, stepping ratio and run length of the NOD motor.

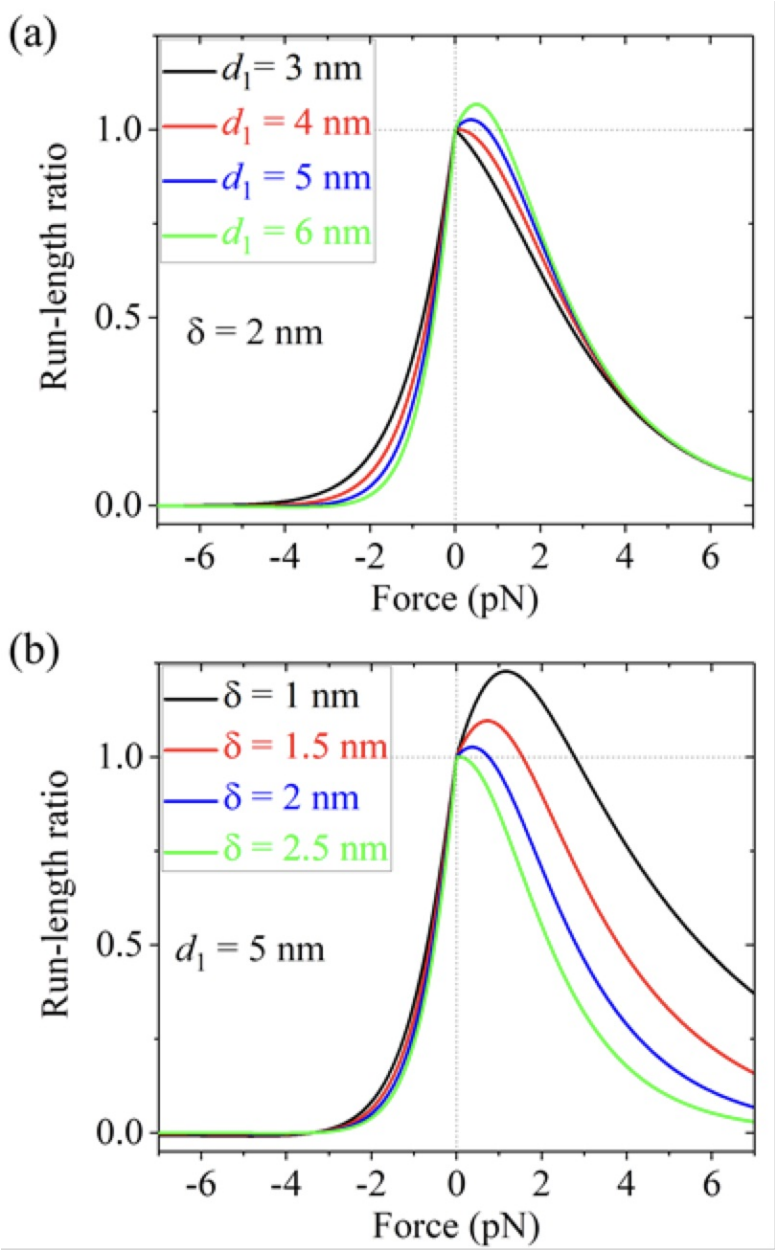

Fig. 5. Theoretical results of ratio of run length under load to that under no load versus load for NOD motor obtained on the basis of Model 3. (a) Results for different values of d_1 and fixed $\delta = 2$ nm. (b) Results for different values of δ and fixed $d_1 = 5$ nm.

4. Discussion

4.1. Comparison between Model 3 for dimerized NOD and the previously proposed model for dimeric kinesin-1

Model 3 for the kinesin-10 NOD motor is similar to the model proposed previously for the kinesin-1 motor[15][33]. The prominent difference between the two models is that in the latter the NL docking can occur and a high affinity is present between the detached head and the MT-bound head before its NL docking [34], whereas in the former no NL docking can occur and no high affinity is present between the two heads.

In the latter model for the kinesin-1, the presence of the high affinity between the two heads can explain well prior biochemical data showing that upon the kinesin-1 dimers with both heads bound by ADP mixing with MT only half fraction of ADPs are released and the addition of ATPs leads to the release of the other half fraction of ADPs [35], as described as follows. Upon a kinesin-1 dimer with both heads bound by ADP mixing with MT, one ADP-head binds to MT with the affinity E_{w2} and the other ADP-head that binds strongly to the MT-bound head cannot bind to MT. Since for the kinesin-1 head ADP release cannot occur without the stimulation of MT, only the MT-bound head can release its ADP. This explains that only half fraction of ADPs can be released. After the addition of ATPs, ATP binding to the nucleotide-free MT-bound head induces a large conformational change of the head, inducing its NL docking and reducing greatly its binding energy to the other detached ADP-head [34]. Thus, the detached ADP-head becomes able to bind to MT, releasing its ADP. This explains the release of the other half fraction of ADPs.

During the processive stepping of a kinesin-1 dimer, the presence of the high affinity between the two heads can lead to the occasional occurrence of the period when only one head in ADP state binds weakly to MT with the very small affinity E_{w1} and that with the small affinity E_{w2} while the other detached head in ADP state binds strongly to the MT-bound head [33]. During the period with the affinity E_{w1} the dimer can dissociate from MT very easily due to E_{w1} being very small although the lifetime of the period (equal to tr) is very short [33]. During the period with the affinity E_{w2} the dimer can dissociate with a non-small probability due to the lifetime of the period (equal to ADP release time) being not very short [33]. By contrast, in Model 3 for the dimerized NOD motor the absence of the high affinity between the two heads can only lead to the period when only one head of the dimer binds weakly to MT (with the affinity E_{w2}) being so short (shorter than 10 μs [30]) that the probability for the dimer to dissociate from MT during the period is very small compared to that during the period when both heads bind weakly to MT with the total affinity $2E_{w2}$.

As seen in Eq. (3), under a near-zero load P_E approaches 0.5 for the dimerized NOD motor. It is interesting to discuss why the dimerized NOD motor does not make use of the NL docking to facilitate the forward movement and thus gives P_E approaching 1. The prior biochemical data showed that the NL docking of the kinesin-1 head can take place with a timescale of 1 ms (equal to the inverse of the NL-docking rate that is larger than 800 s^{-1} [36]). Since the time for the trailing head to diffuse to the front tubulin is much shorter than 1 ms, for the kinesin-1 to make use of the NL docking to facilitate the forward movement, it is required that a high affinity is present between the detached head and the MT-bound head before its NL docking [33]. Assume that the NL docking of the NOD head can also occur with a timescale of 1 ms and before the NL docking the MT-bound head also has a high affinity to the detached head so that the detached head cannot

bind to MT, as in the case of kinesin-1. Then, it is expected that for the NOD motor in every step a time period of about 1 ms can occur, when only one head in nucleotide-bound state binds weakly to MT with the affinity E_{w2}. During this period of about 1 ms the NOD motor can dissociate from MT with a non-small probability by overcoming the weak affinity E_{w2}. Thus, the NOD motor can only have a low processivity. The movement of the NOD motor toward the plus end of MT with a non-low processivity is necessary for its biological function of driving chromosome arms away from spindle poles [8][37][38]. To ensure the high processivity, it is required that the time period when only one head binds weakly to MT with the small affinity E_{w2} is as short as possible, which can be realized by adopting the mechanism that the high affinity is absent between the detached head and the MT-bound head, as proposed in Model 3.

Moreover, if the dimerized NOD motor makes use of the NL docking to facilitate the forward movement, like kinesin-1, it is expected that after the dimerized NOD motor reaching the MT plus end it would dissociate rapidly from the MT end due to the large energy change of the NL docking and the associated large conformational change of the head, as recent studies showed [39]. By contrast, for the dimerized NOD motor with no NL docking, i.e., with zero energy change of the NL docking and the associated large conformational change of the head, after it reaching the MT plus end it would reside there for a long time, as the recent studies showed [39], thus performing its function at the MT end.

4.2. Dimerized KID has the similar chemomechanical coupling pathway to dimerized NOD

In this work, we show that the chemomechanical coupling pathway of the dimerized NOD can be reasonably described by Model 3 (Fig. 3). It is proposed here that another species of chromokinesin, human KID, after dimerization shows the similar chemomechanical coupling pathway to the dimerized NOD.

The available biochemical data showed that a KID head in both nucleotide-free and AMPPNP states has a high affinity to MT while in ADP state has a relatively low affinity [9]. Thus, similar to element (i) for Model 3 described in Section 2.3 for the NOD, the element for the KID is modified as follows. (i) The KID head in nucleotide-free, ATP and ADP.Pi states has a strong interaction with MT while in ADP state has a relatively weak interaction with MT. This feature for the KID head is similar to that for the kinesin-1 head. The strong interaction induces large conformational changes of the local tubulin while the relatively weak interaction induces little conformational changes of the local tubulin. The KID head in ADP state has a much weaker affinity (E_{w1}) to the local tubulin having the large conformational changes than the weak affinity (E_{w2}) to other tubulins having no large conformational changes. Thus, after the MT-bound head releases Pi, a very short time t_r (in the order of μs) is present when the ADP-head has the very weak affinity E_{w1} to the local tubulin and in t_r the affinity of the ADP-head to the local tubulin changes to E_{w2}. Element (ii) for the KID head is the same as that for the NOD head. Namely, the KID head with the backward-directed NL has a much slower rate of ATP transition to ADP than the head with the forward-directed NL. In addition, no NL docking occurs and no strong affinity is present between the two heads for the dimerized KID, as in the case for the dimerized NOD.

The model for the dimerized KID can be schematically illustrated in Fig. 6, where we also focus on saturating ATP and for simplicity ATP represents both ATP and ADP.Pi. We begin the stepping pathway with the trailing and leading heads in ATP state bound strongly to tubulins II and III, respectively (Fig. 6a). First, consider ATP transition to ADP in the trailing

head (Fig. 6b). The trailing head detaches from tubulin II by overcoming the very small E_{w1} and diffuses forward (Fig. 6c). In the short time t_r, the deformed tubulin II returns elastically to the normal one without the large conformational changes (Fig. 6d). The detached head can diffuse forward further and bind to tubulin IV with the affinity E_{w2}, which is followed by rapid ADP release and instant ATP binding (Fig. 6e). From Fig. 6b, the detached head can also diffuse backward and bind to tubulin II with the affinity E_{w2}, which is followed by rapid ADP release and instant ATP binding (Fig. 6a). From Fig. 6a to d to e, a forward step of the dimer was made by consuming one ATP. From Fig. 6a to d to a, no movement of the dimer was made although one ATP is consumed. Second, consider ATP transition to ADP in the leading head (Fig. 6f). The leading head detaches from tubulin III and diffuses backward (Fig. 6g). In the short time t_r, the deformed tubulin III returns elastically to the normal one without the large conformational changes (Fig. 6h). The detached head can diffuse backward further and bind to tubulin I with the affinity E_{w2}, which is followed by rapid ADP release and instant ATP binding (Fig. 6i). From Fig. 6h, the detached head can also diffuse forward and bind to tubulin III with the affinity E_{w2}, followed by rapid ADP release and instant ATP binding (Fig. 6a). From Fig. 6a to h to i, a backward step of the dimer was made by consuming one ATP. From Fig. 6a to h to a, no movement of the dimer was made although one ATP is consumed.

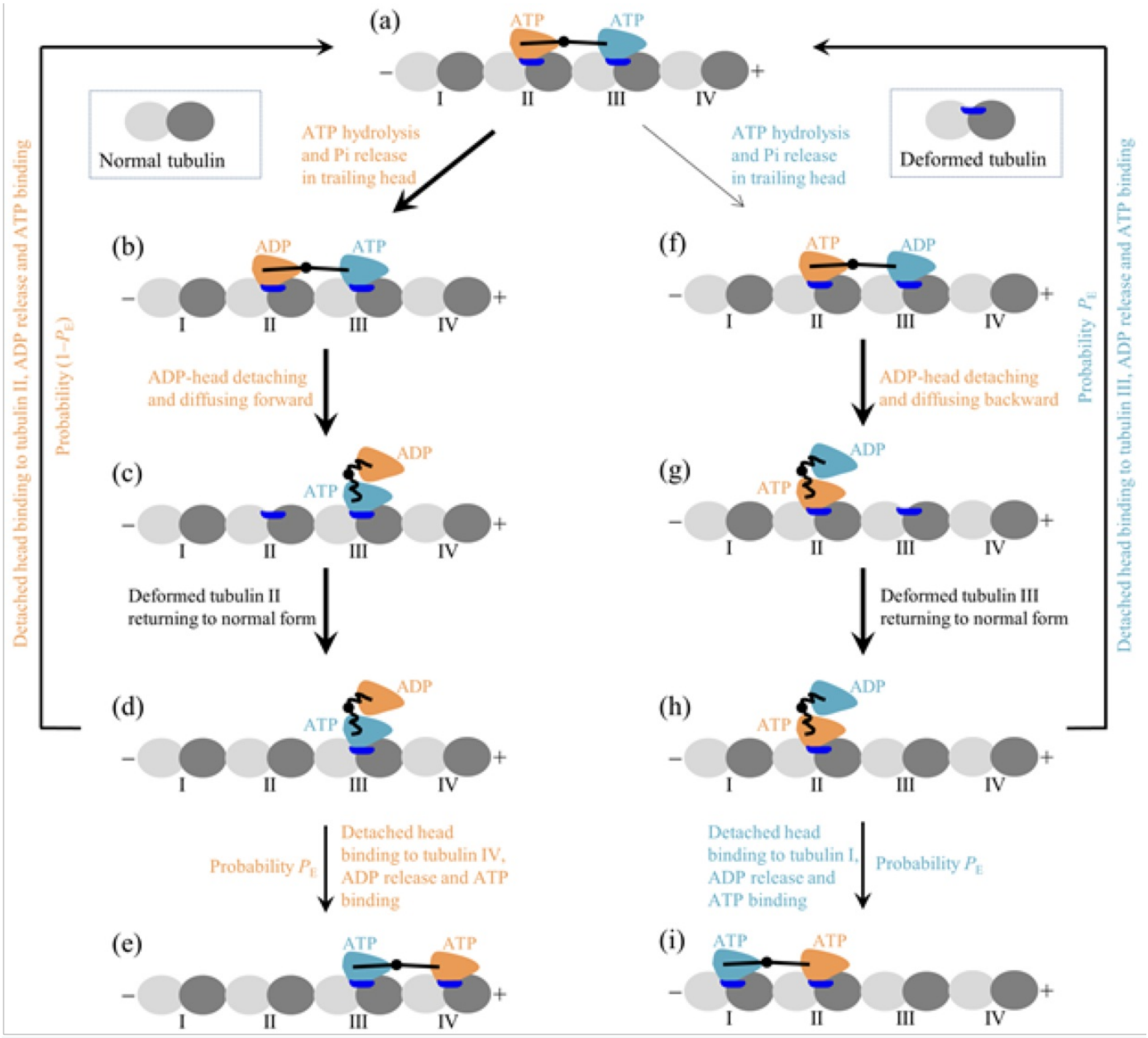

Fig. 6. Model for stepping of dimerized KID motor. (a – i) The chemomechanical coupling pathway at saturating ATP (see Section 4.2 for detailed descriptions). For simplicity, both ATP and ADP.Pi states are represented by ATP state. The thickness of the arrow indicates the relative magnitude of the probability of the transition between two states connected by the arrow under no load.

It is noted here that in the model of Fig. 6 even if the NL docking can take place, since the time period from the detachment of the head from MT to the re-binding of the detached head to MT is much shorter (in the order of 10 μs) than the inverse of NL-docking rate (in the order of ms), during the time period the NL docking of the MT-bound ATP-head cannot occur. The NL docking of the trailing head takes place in the two-heads-bound state. Thus, even if the NL docking can occur, it plays no role in the stepping of the dimerized KID.

The pathway of Fig. 6 for the dimerized KID is similar to that of Fig. 3 for the dimerized NOD. Thus, the KID motor would show the similar dynamics to the NOD motor, as shown in Figs. 4 and 5. In addition, since both the curve of velocity versus load and that of detachment time versus load for the chromokinesin NOD and KID dimers of kinesin-10 family are

similar to those for the chromokinesin CENP-E dimer of kinesin-7 family (see Section 3.2), it is expected that the two families of chromokinesin motors show the similar chemomechanical coupling mechanism. In more details, considering that the CENP-E, like the KID, has a high binding energy to MT in nucleotide-free, ATP and ADP.Pi states whereas has a low binding energy in ADP state, it is expected that the CENP-E dimer has the same chemomechanical coupling pathway as the KID dimer, as shown schematically in Fig. 6.

5. Conclusions

To understand the physical mechanism of the dimerized NOD motor moving on MT, we considered three models, Model 1, Model 2 and Model 3. Model 1 and Model 2 are analogous to the prevailing model presented in the literature for the kinesin-1 motor, where NL docking of the leading ATP-head provides the force to drive the forward movement of the trailing head relative to the leading one. It is analyzed that Model 1 and Model 2 lead to the nonprocessivity for the dimerized NOD due to the weak interaction between the leading ATP-head and MT, which is contrary to the available experimental results. Model 3 is derived from the model for the kinesin-1 motor proposed before, where the forward movement of the trailing head relative to the leading one is via the Brownian ratchet mechanism. However, Model 3 for the dimerized NOD is different from the latter model for the kinesin-1, in that in Model 3 no NL docking occurs whereas in the latter model for the kinesin-1 the NL docking plays an assisting role in the forward movement. On the basis of Model 3 the theoretical results explain well the processive movement of the dimerized NOD motor. To further verify Model 3, in future it is hoped to test the predicted results (Figs. 4 and 5) by using the singe molecule optical trapping methods.

Declarations

- **Competing interests:** The author declares no competing interests.
- **Ethical approval:** The study is purely theoretical and does not involve any experiment with animals that would require ethical approval.
- **Informed consent:** The study does not involve any participants that would require to give their informed consent.
- **Author contribution:** PX designed the research, performed the research and wrote the manuscript.

References

1. ^*Lawrence C.J., et al. (2004) A standardized kinesin nomenclature. J. Cell Bio. 167, 19–22.*
2. ^*Miki H., Okada Y., Hirokawa N. (2005) Analysis of the kinesin superfamily: insights into structure and function. Trends Cell Biol. 15, 467–476.*
3. a, b, c, d*Afshar K., Barton N.R., Hawley R.S., Goldstein L.S. (1995) DNA binding and meiotic chromosomal localization of the Drosophila nod kinesin-like protein. Cell 81, 129–138.*
4. a, b, c, d*Afshar K., Scholey J., Hawley R.S. (1995) Identification of the chromosome localization domain of the*

Drosophila nod kinesin-like protein. J. Cell Biol. 131, 833–843.

5. [a, b, c, d, e, f, g, h, i, j, k] *Cochran J., Sindelar C., Mulko N., Collins K., Kong S., Hawley R., Kull F. (2009) ATPase cycle of the nonmotile kinesin NOD allows microtubule end tracking and drives chromosome movement. Cell 136, 110–122.*
6. [^] *Matthies H., Baskin R., Hawley R. (2001) Orphan kinesin NOD lacks motile properties but does possess a microtubule-stimulated ATPase activity. Mol. Biol. Cell 12, 4000–4012.*
7. [^] *Cui W., Hawley R.S. (2005). The HhH2/NDD domain of the Drosophila Nod chromokinesin-like protein is required for binding to chromosomes in the oocyte nucleus. Genetics 171, 1823–1835.*
8. [a, b, c, d] *Cane S., Ye A.A., Luks-Morgan S J., Maresca T. J. (2013) Elevated polar ejection forces stabilize kinetochore-microtubule attachments. J. Cell Biol. 200, 203–218.*
9. [a, b, c, d, e, f, g, h, i] *Walker B.C., Tempel W., Zhu H., Park H., Cochran J.C. (2019) Chromokinesins NOD and KID use distinct ATPase mechanisms and microtubule interactions to perform a similar function. Biochemistry 58, 2326–2338.*
10. [a, b] *Cross R.A. (2016) Mechanochemistry of the kinesin-1 ATPase. Biopolymers 105, 476-482.*
11. [a, b] *Sosa H., Peterman E.J.G., Moerner W.E., Goldstein L.S.B. (2001) ADP-induced rocking of the kinesin motor domain revealed by single-molecule fluorescence polarization microscopy. Nature Struc. Biol. 8, 540-544.*
12. [a, b, c, d] *Ye A.A., Verma V., Maresca T.J. (2018) NOD is a plus end-directed motor that binds EB1 via a new microtubule tip localization sequence. J. Cell Biol. 217, 3007–3017.*
13. [^] *Soppina, V., Norris, S. R., Dizaji, A. S., Kortus, M., Veatch, S., Peckham, M., Verhey, K. J. (2014) Dimerization of mammalian kinesin-3 motors results in superprocessive motion, Proc. Natl. Acad. Sci. U. S. A. 111, 5562-5567.*
14. [^] *Guo S.-K., Shi, X.-X., Wang P.-Y., Xie, P. (2019) Run length distribution of dimerized kinesin-3 molecular motors: comparison with dimeric kinesin-1. Sci. Rep. 9, 16973.*
15. [a, b, c, d] *Xie P. (2021) Insight into the chemomechanical coupling mechanism of kinesin molecular motors. Commun. Theor. Phys. 73, 057601.*
16. [a, b] *Vale R.D., Milligan R.A. (2000) The way things move: looking under the hood of molecular motor proteins. Science 288, 88–95.*
17. [a, b] *Endow S.A., Barker D.S. (2003) Processive and nonprocessive models of kinesin movement. Annu. Rev. Physiol. 65, 161–175.*
18. [a, b] *Klumpp L.M., Hoenger A., Gilbert S.P. (2004) Kinesin's second step. Proc. Natl. Acad. Sci. U.S.A. 101, 3444–3449.*
19. [a, b] *Rosenfeld S.S., Fordyce P.M., Jefferson G.M., King P.H., Block S.M. (2003) Stepping and stretching: how kinesin uses internal strain to walk processively. J. Biol. Chem. 278, 18550–18556.*
20. [a, b] *Schief W.R., Howard J. (2001) Conformational changes during kinesin motility. Curr. Opin. Cell Biol. 13, 19–28.*
21. [a, b, c] *Mori T., Vale R.D., Tomishige, M. (2007) How kinesin waits between steps. Nature 450, 750–754.*
22. [a, b] *Xie P. (2023) Effect of the neck linker on processive stepping of kinesin motor. Biophysica 3, 46–68.*
23. [^] *Morikawa M., Yajima H., Nitta R., Inoue S., Ogura T., Sato C., Hirokawa N. (2015) X-ray and cryo-EM structures reveal mutual conformational changes of kinesin and GTP-state microtubules upon binding. EMBO J. 34, 1270–1286.*
24. [a, b, c] *Shi X.-X., et al. (2018) Investigating role of conformational changes of microtubule in regulating its binding affinity to kinesin by all-atom molecular dynamics simulation. Proteins 86, 1127–1139.*
25. [a, b, c] *Shi X.-X., Wang P.-Y., Chen H., Xie P. (2021) Studies of conformational changes of tubulin induced by interaction*

with kinesin using atomistic molecular dynamics simulations. Int. J. Mol. Sci. 22, 6709.

26. [a, b, c]*Cao L., Wang W., Jiang Q., Wang C., Knossow M., Gigant B. (2014) The structure of apo-kinesin bound to tubulin links the nucleotide cycle to movement. Nat. Comm. 5, 5364.*
27. [^]*Nitta R., Okada Y., Hirokawa N. (2008) Structural model for strain-dependent microtubule activation of Mg-ADP release from kinesin. Nat. Struct. Mol. Biol. 15, 1067–1075.*
28. [a, b]*Gudimchuk N., Tarasovetc E.V., Mustyatsa V., Drobyshev A.L., Vitre B., Cleveland D.W., Ataullakhanov F.I., Grishchuk E.L. (2018) Probing mitotic CENP-E kinesin with the tethered cargo motion assay and laser tweezers. Biophys. J. 114, 2640–2652.*
29. [a, b]*Iemura K., Tanaka K. (2015) Chromokinesin Kid and kinetochore kinesin CENP-E differentially support chromosome congression without end-on attachment to microtubules. Nat. Commun. 6, 6447.*
30. [a, b]*Guo S.-K., Wang P.-Y., Xie P. (2017) A model of processive movement of dimeric kinesin. J. Theor. Biol. 414, 62-75.*
31. [^]*Uemura S., Kawaguchi K., Yajima J., Edamatsu M., Toyoshima Y.Y., Ishiwata S.I. (2002) Kinesin–microtubule binding depends on both nucleotide state and loading direction. Proc. Natl. Acad. Sci. U. S. A. 99, 5977-5981.*
32. [^]*Wang et al. (2022) Investigation of the structural and dynamic basis of kinesin dissociation from microtubule by atomistic molecular dynamics simulations. Chin. Phys. B 31, 058702.*
33. [a, b, c, d, e]*Xie P. (2020) Theoretical analysis of dynamics of kinesin molecular motors. ACS Omega 5, 5721–5730.*
34. [a, b]*Shi X.-X., Guo S.-K., Wang P.-Y., Chen H., Xie P. (2020) All-atom molecular dynamics simulations reveal how kinesin transits from one-head-bound to two-heads-bound state. Proteins 88, 545–557.*
35. [^]*Hackney D.D. (1994) Evidence for alternating head catalysis by kinesin during microtubule-stimulated ATP hydrolysis. Proc. Natl. Acad. Sci. U. S. A. 91, 6865-6869.*
36. [^]*Rosenfeld S.S., Jefferson G.M., King P.H. (2001) ATP reorients the neck linker of kinesin in two sequential steps. J. Biol. Chem. 276, 40167-40174.*
37. [^]*Ke K., Cheng J., Hunt A.J. (2009) The distribution of polar ejection forces determines the amplitude of chromosome directional instability. Curr. Biol. 19, 807–815.*
38. [^]*Li C., Xue C., Yang Q., Low B.C., Liou Y.-C. (2016) NuSAP governs chromosome oscillation by facilitating the Kid-generated polar ejection force. Nat. Commun. 7, 10597.*
39. [a, b]*Xie P. (2023) Determinant factors for residence time of kinesin motors at microtubule ends. J. Biol. Phys. 49, 77–93.*